European Journal of Clinical and Experimental Medicine

ONLINE FIRST

Authors: Ahmed F. Abed Mansoor, Ahmed Rahmah Abu-Raghif, Hayder Ridha-Salman, Furqan Mohammed Al-Asady, Maytham Razaq Shleghm, Muataz Naeem Hussein

Article type: Original Article

Received: 5 September 2025

Accepted: 10 December 2025

Published online: 27 January 2026

eISSN: 2544-1361

Eur J Clin Exp Med

doi:10.15584/ejcem.2026.1.23

Pulmonoprotective effect of carnosol on LPS-induced cytokine storm model in mice

Ahmed F. Abed Mansoor [1], Ahmed Rahmah Abu-Raghif [2], Hayder Ridha-Salman [3], Furqan Mohammed Al-Asady [4,5], Maytham Razaq Shleghm [1], Muataz Naeem Hussein [2]

[1] Department of Pharmacology and Toxicology, College of Pharmacy- National University of Science and Technology, An Nasiriyah, Dhi Qar, Iraq

[2] Al-Nahrain University, College of Medicine, Department of Pharmacology, Baghdad, Iraq

[3] Al-Mustaqbal University, College of Pharmacy, Hilla, Babylon, Iraq

[4] University of Hilla, College of Pharmacy, Babylon, Iraq

[5] University of Babylon, Hammurabi College of Medicine, Hillah, Iraq

Corresponding author: Hayder Ridha-Salman, e-mail: hayder80.ridha@gmail.com; haider.redha@uomus.edu.iq

ORCID

AFAM: https://orcid.org/0009-0002-9466-5929

ARA-R: https://orcid.org/0000-0003-4514-3892

HR-S: https://orcid.org/0000-0003-1594-4883

FMA-A: https://orcid.org/0000-0002-3728-8330

MRS: https://orcid.org/0009-0005-7596-7579

MNH: https://orcid.org/0009-0002-0027-7387

ABSTRACT

Introduction and aim. The cytokine storm represents a severe hyperinflammatory response that can lead to acute lung injury and organ failure. Carnosol, a phenolic diterpene derived from *Rosmarinus officinalis*, exhibits documented antioxidant and anti-inflammatory properties. The aim was to evaluate the effects of carnosol, alone and in combination with methylprednisolone acetate (MPA), in a lipopolysaccharide (LPS)-induced cytokine storm model in mice.

Material and methods. Sixty male mice were randomly assigned to six groups: control, lipopolysaccharide (LPS), vehicle, carnosol (120 mg/kg), methylprednisolone acetate (50 mg/kg), and combined carnosol plus methylprednisolone acetate (half doses). Treatments were administered for seven days following LPS induction. Pulmonary concentrations of interleukin-1 beta (IL-1β), interleukin-6 (IL-6), and tumor necrosis factor alpha (TNF-α) were quantified using enzyme-linked immunosorbent assay, and lung histopathology was evaluated.

Results. Lipopolysaccharide administration significantly increased pulmonary cytokine levels compared with controls (IL-1β: 85.8±13.5 vs. 11.5±3.8 pg/g; IL-6: 93.0±8.5 vs.16.6±4.8 pg/g; TNF-α: 144.4±10.1 vs.18.6±0.01 pg/g; all $p<0.05$). Treatment with carnosol significantly reduced IL-1β, IL-6, and TNF-α levels compared with the LPS group ($p<0.05$). The combined carnosol and methylprednisolone acetate therapy produced the greatest cytokine attenuation (e.g. IL-6: 24.6±1.8 pg/g vs. LPS; $p<0.05$) and was associated with the most pronounced improvement in lung histopathological scores ($p<0.05$).

Conclusion. Carnosol attenuates lipopolysaccharide-induced pulmonary inflammation and cytokine overproduction in a murine model. Its combination with methylprednisolone acetate may enhance anti-inflammatory efficacy and allow for glucocorticoid dose reduction. These findings provide preclinical evidence supporting further mechanistic and translational studies.

Keywords. ARDS, carnosol, COVID-19, mouse model, phenolic diterpenes

Introduction

Cytokine storm syndrome is a pathophysiological state of systemic hyper-inflammation caused by uncontrolled release of pro-inflammatory cytokines, which results in tissue damage, organ failure, and high mortality.[1,2] It is initiated by infectious (bacterial endotoxins, viral infections) and non-infectious stimuli (malignancy, autoimmunity).[3-5] In the context of severe inflammation, an uncontrolled release of cytokines is associated with complications, including acute respiratory distress syndrome (ARDS), multiple organ failure, and death.[6-8] Increased concentrations of key mediators such as interleukin (IL)-1β, IL-6, and tumor necrosis factor (TNF)-α are constantly correlated with disease severity and bad prognosis.[9-11]

Lipopolysaccharide (LPS) – abundant in the Gram-negative bacterial membrane – is a popular tool for modeling cytokine storms, as it efficiently stimulates innate immunity and induces a strong production of an excessive amount of cytokines.[12-14] LPS-mediated inflammation is transmitted by well-defined signaling pathways culminating in transcriptional induction of pro-inflammatory cytokines with consequent systemic inflammatory damage. While these pathways have been well-characterized in the literature, their prolonged activation is a central mechanism underlying cytokine storm pathology.[15]

Glucocorticoids have represented a mainstay to treat severe inflammatory diseases because of their powerful immunosuppressive and anti-inflammatory activities.[16,17] Synthetic glucocorticoids, including methylprednisolone acetate (MPA), can efficiently inhibit the production of cytokines and immune cell invasion. These are, however, associated with immunosuppression and an increased risk of infection as well as decreased tissue repair and metabolic derangement.[18,19] Unfortunately, long-term or high-dose glucocorticoid therapy is also connected with severe side effects. These shortcomings highlight the demand for alternative or adjuvant anti-inflammatory remedies able to effectively suppress cytokine storms with less systemic toxicity.

Natural products can be considered as an important reservoir of bioactive compounds possessing versatile pharmacological activities.[20,21] Carnosol, a natural phenolic diterpene found in rosemary (*Rosmarinus officinalis*), sage, and other herbs, possesses robust antioxidant, anti-inflammatory, anti-proliferative, and immune-modulating activities.[22] Multiple preclinical investigations have revealed carnosol anti-inflammatory efficacy in a variety of animal models, confirming its capacity to inhibit inflammatory mediators, modify immune cell function, and ameliorate oxidative stress.[23] Although these outcomes corroborate its anti-inflammatory capacity, previous studies have primarily been based on experimental disease or endpoints that may not allow for direct comparison with established anti-inflammatory therapies. However, to the best of our knowledge, there have been no in vivo studies that systematically compare the anti-inflammatory activity of carnosol with typical glucocorticoid compounds as well as attempt to evaluate their combined effects under LPS-induced cytokine storm conditions. This gap needs to be addressed to provide critical insight into whether carnosol can be utilized as a complementary or alternative treatment for controlling exaggerated hyperinflammatory responses.

Aim

Therefore, the aim of this study was to assess the anti-inflammatory effects of carnosol alone and in combination with methylprednisolone acetate by using the LPS-driven cytokine storm model in vivo. Direct comparison of these interventions aims to clarify the therapeutic potential and translational importance from preclinical studies for carnosol as a molecule dampening in a setting of exacerbated systemic inflammation.

This research fills in these gaps by clarifying the core hypothesis that carnosol mitigates the LPS-driven cytokine storm in mice and prevents lung damage, with the added likelihood that its combined action with MPA could permit glucocorticoid dosage reductions while offering safer anti-inflammatory therapy. The investigation's primary endpoint was to evaluate pulmonary tissue concentrations of IL-1β, IL-6, and TNF-α 24 hours after LPS injections. The secondary endpoints are lung histopathology scores.

Material and methods

Carnosol, MPA, and LPS were obtained from Sigma Aldrich Chemical Company (St. Louis, MO, USA). Dimethyl sulfoxide (DMSO) was acquired from Chem-Lab NV (Zedelgem, Belgium). Formaldehyde was supplied from Sinopharm Chemical Reagent Co., Ltd. Commercial enzyme-linked immunosorbent assay (ELISA) kits for mouse TNF-α, IL-1β, and IL-6 were purchased from Sunlong Biotech Co., Ltd. Hematoxylin and eosin (H&E) staining reagents were procured from BDH Chemicals (Poole, UK).

Reagents and kits are reported as per the standardized company name, city, and country.

Experimental animals and ethical consideration

A total of 60 male Swiss albino mice (pathogen-free, aged 7–8 weeks, weighing 25–30 g) were used in this study. All animals were housed under controlled laboratory conditions, including a 12-hour light/dark cycle and an ambient temperature maintained at 18–22°C. Standard rodent chow and water were provided ad libitum. A 14-day acclimatization period was allowed prior to the commencement of the experiments. No animals satisfied the humane endpoint criteria; hence, no exclusions were imposed. All experimental procedures were approved by the Animal Ethics Committee of Al-Nahrain University, College of Medicine (approval date: November 21, 2021; Approval No. 20215951), and adhered to the guidelines for the care and use of laboratory animals.

Sample size calculation, randomization, and blinding

The sample size was determined for the primary endpoint of expected differences in pulmonary TNF-α levels with a statistical power of 80% at a significance level of α=0.05. The minimum number needed was 8 animals for each study group; we used 10 mice per group to allow for biological variability and probable losses.

Mice were arbitrarily assigned into 6 groups (n = 10 per group) employing a software-generated randomization sequence. Staff performing the biochemical analyses (ELISA assays and quantitation) were blinded to group assignment throughout sample processing, assay execution, and data analysis. Histopathological analysis and scoring were performed in a blinded manner by an experienced histopathologist during slide reading and scoring.

Experimental design

For induction of a cytokine storm, mice were challenged with a single intraperitoneal (i.p.) injection of LPS (5 mg/kg). Therapeutic interventions started 1 h after LPS and proceeded once per day for 7 days as follows:

- Control group (Healthy): received no treatment.
- LPS group (Induction): injected with LPS alone (5 mg/kg, i.p.).[24]
- DMSO (Vehicle) group: received LPS then 1% DMSO (0.3 mL, i.p.).[25]
- Methylprednisolone group (MPA): were given LPS and then treated with MPA (50 mg/kg, i.p.).[26]
- Carnosol group: challenged with LPS and then treated with carnosol (120 mg/kg, i.p.).[27]
- Carnosol + Methylprednisolone combination group (Carnosol+MPA): injected with LPS, and after 1 h obtained carnosol (60 mg/kg) and MPA (25 mg/kg), independently, via i.p. administration.

The carnosol dose (120 mg/kg) and MPA (50 mg/kg) were selected based on previously published experimental studies demonstrating therapeutic efficacy without evident toxicity in rodent models.[28]

These established doses were adopted to ensure comparability with existing literature and to minimize the risk of dose-related adverse effects. Figure 1 displays a simplified representation of the research methodology and treatment schedule.

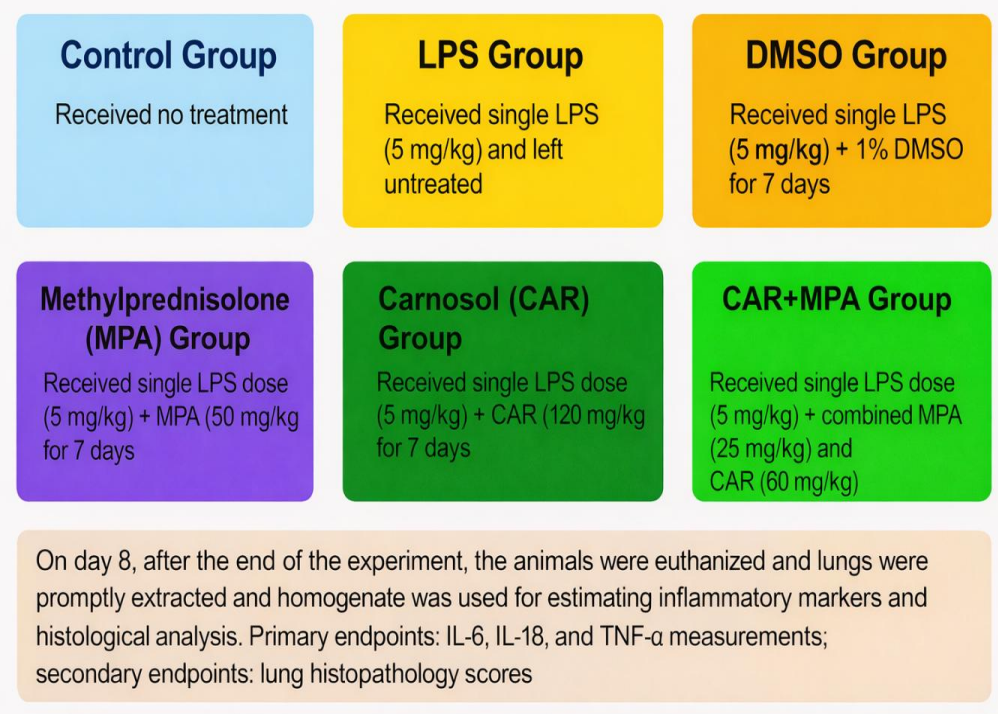

Fig. 1. Schematic diagram illustrating the experimental design and treatment timeline

Formulation of tested agents

Carnosol was dissolved in a 1% DMSO and diluted with sterilized saline to achieve an ultimate working concentration of 10 mg/mL Dosing volumes were estimated according to body weight for delivering 120 mg/kg (0.36 mL) of carnosol. MPA was mixed in 1% DMSO and subsequently diluted with sterilized saline to provide a 5 mg/mL working solution and was delivered intraperitoneally at 50 mg/kg using individually calculated volumes (0.3 mL). Carnosol and MPA were regularly injected intraperitoneally spanning a period of 7 days to assure continuous systemic exposure and guarantee predictable therapeutic actions throughout the LPS-driven inflammatory stages. In the combination treatment group, carnosol and MPA were given separately through the i.p. route with no premixed preparation.

Cytokine storm model (induction protocol)

LPS stock solution was prepared freshly according to the manufacturer's protocol by dissolving LPS powder in sterile normal saline solution and then mixing by vortex before use.[29] A cytokine storm was elicited by a single i.p. injection of LPS (5 mg/kg).[21,30]

Animal euthanasia and lung tissue homogenization

On day 8, after the last dosage of medications was administered, the animals were euthanized with an intraperitoneal injection of ketamine (80 mg/kg) and xylazine (8 mg/kg) for ensuring the complete suppression of pain reflexes before sacrificing. The chest cavity was cautiously opened, and the lungs were promptly evacuated. After that, the lung tissues were split into two parts. One part was fixed in 10% neutral-buffered formalin for the histopathological study, and the other part was softly cleansed with ice-cold sterilized saline, wiped dry with a paper towel, and homogenized in phosphate-buffered saline at a 10% w/v mixture via a tissue homogenizing device. The pulmonary homogenates were spun out at 10,000×g for 15 minutes at 4°C, and the resultant supernatants were gathered for ELISA analyses.

Cytokine measurement methodology

The concentrations of TNF-α, IL-1β, and IL-6 in the lung tissue samples were measured by ELISA with commercially available kits according to the manufacturer's instructions. All measurements were carried out in a double-blind system.[31,32] The optical density was read at 450 nm, and cytokine concentrations were determined from standard curves and expressed as pg per mg of tissue.[33,34]

Histopathological examination

Lung tissues were fixed in 10% neutral-buffered formalin for at least 24 hours to preserve morphology, then processed through graded ethanol concentrations, cleared with xylene, and embedded in paraffin wax.[35,36] Paraffin blocks were sectioned at 4–5 µm using a rotary microtome. Sections were floated in a warm water bath to remove folds, mounted onto clean slides, and air-dried at 37°C. Standard H&E staining was used to assess tissue architecture. Slides were deparaffinized, rehydrated, stained with hematoxylin, differentiated in acid alcohol, blued, and counterstained with eosin.[31,37] After dehydration and clearing, sections were mounted with coverslips. Histopathological evaluations and scoring systems were conducted by a single experienced histopathologist who was blinded to group assignments. All the specimens were examined microscopically at various magnifications (10×, 40×).

Scoring of histopathological changes

A partially quantitative evaluation procedure with an array of 0 to 4 was adopted to assess histopathology abnormalities dependent on alveolar morphology, interstitial inflammation, edema, and hemorrhaging at 10× and 40× amplification. Grade 0 (0% negative) meant that there was no visible injury, and the lung structure was normal. Grade 1 (1–33% mild positive) illustrated mild alveolar wall thickenings and minimal involvement of inflammatory cells. Grade 2 displayed modest swelling, inflammatory invasion, and noticeable alveolar septal thickenings (33–66% moderate positive). Severe septal thickenings, intense

inflammatory migration, and substantial edema or hemorrhage were indicative of grade 3. Grade 4 (66–100% severely positive) revealed extensive bleeding, significant inflammatory cell infiltration, alveolar collapse, and diffuse alveolar damage. Scale bars were used to illustrate typical features in representative photos for each grade. Multiple non-overlapping microscopy regions from each tissue segment were examined and averaged for calculating sample-level grade. All portions were evaluated separately by a specialist histopathologist who was totally unaware of the treatment assignment. Recorded lesion outcomes were also matched to a recognized acute lung damage grading tool for comparison with prior research.[38]

Analytical statistics

Data were statistically analyzed through SPSS software (IBM Corp., Armonk, NY, USA) and described as mean ± standard deviation (SD). Data were tested for normality of distribution by the Shapiro–Wilk test before statistical examination. One-way analysis of variance (ANOVA) was used with normality and homogeneity of variances checked, and Tukey's post-hoc test for comparison between multiple groups. Values of $p<0.05$ were considered significant.[39]

Results

Preventive effect of tested agents on IL-1β, IL-6, and TNF-α levels

LPS treatment markedly elevated the levels of IL-1β, IL-6, and TNF-α in lung tissues when compared with the healthy control group ($p<0.05$). Such elevations were also evident in the DMSO group ($p<0.05$). In contrast, mice treated with MPA, carnosol, or their combined treatment revealed a remarkable decrement in the pulmonary levels of IL-1β, IL-6, and TNF-α cytokines in comparison to mice treated with LPS or DMSO ($p<0.05$), as detailed in Figures 2–4.

Notably, the carnosol+MPA combination group produced the best results, demonstrating a substantially greater reduction in IL-6 and TNF-α concentrations than the groups individually treated with MPA or carnosol ($p<0.05$), while IL-1β decline was comparable across all treatment groups (Figures 2–4).

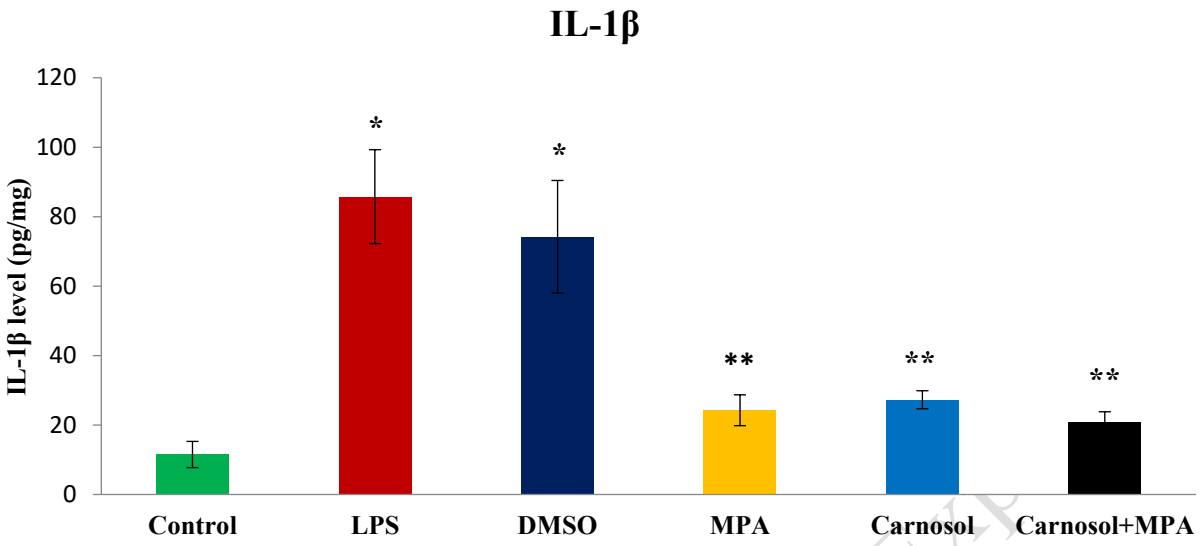

Fig. 2. Impact of the tested agents on IL-1β levels in mouse lung tissue, data are reflected as mean±SD, * – indicates a remarkable difference vs. the control group ($p<0.05$), ** – indicates a remarkable difference vs. the LPS and DMSO groups ($p<0.05$), and # – indicates a remarkable difference vs. the carnosol and/or MPA group ($p<0.05$)

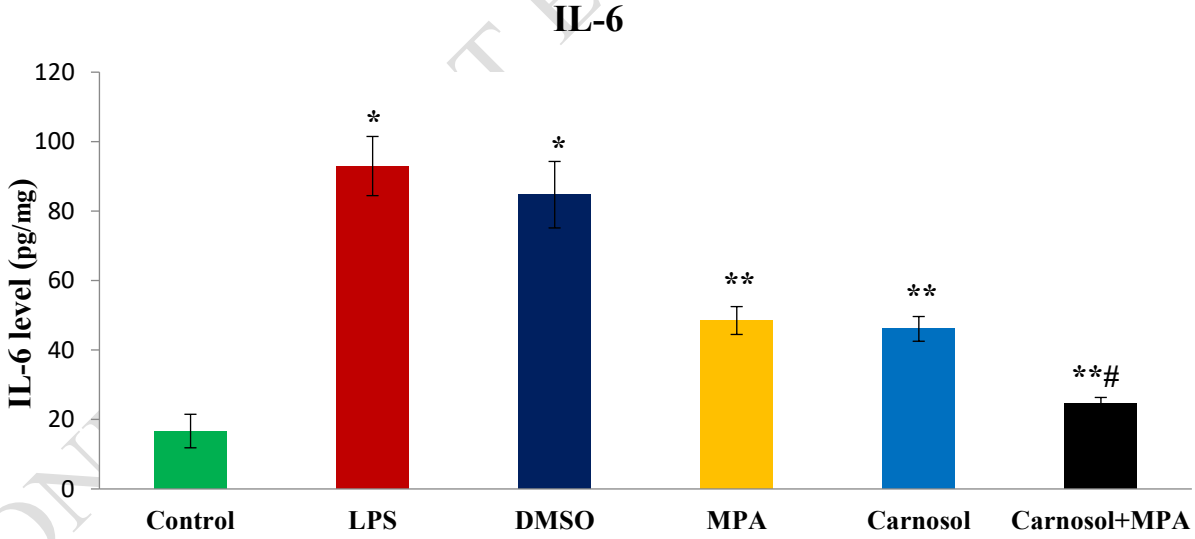

Fig. 3. Impact of the tested agents on IL-6 levels in mouse lung tissue, data are reflected as mean±SD, * – indicates a remarkable difference vs. the control group ($p<0.05$), ** – indicates a remarkable difference vs. the LPS and DMSO groups ($p<0.05$), and # – indicates a remarkable difference vs. the carnosol and/or MPA group ($p<0.05$)

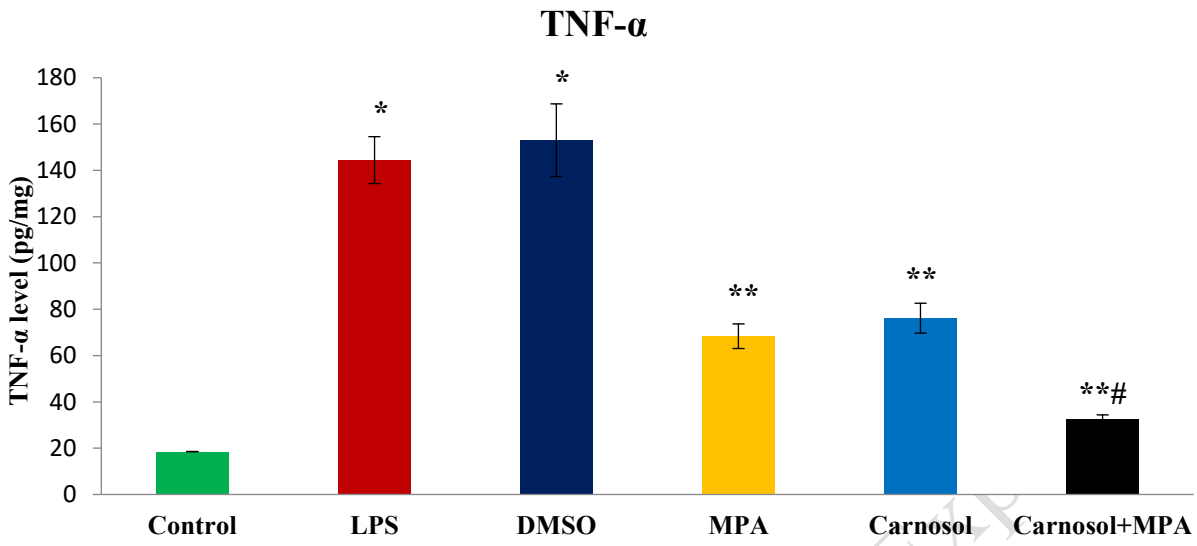

Fig. 4. Impact of the tested agents on TNF-α levels in mouse lung tissue, data are reflected as mean±SD, * – indicates a remarkable difference vs. the control group ($p<0.05$), ** – indicates a remarkable difference vs. the LPS and DMSO groups ($p<0.05$), and # –indicates a remarkable difference vs. the carnosol and/or MPA group ($p<0.05$)

Preventive effect of tested agents on lung histopathological scores

The histopathologic scores of the lungs were significantly higher in the LPS and DMSO groups than those of the healthy control group ($p<0.05$). Treatment with MPA, carnosol, or their combined administration significantly decreased histological scores compared to the LPS and DMSO groups ($p<0.05$) (Figure 5).

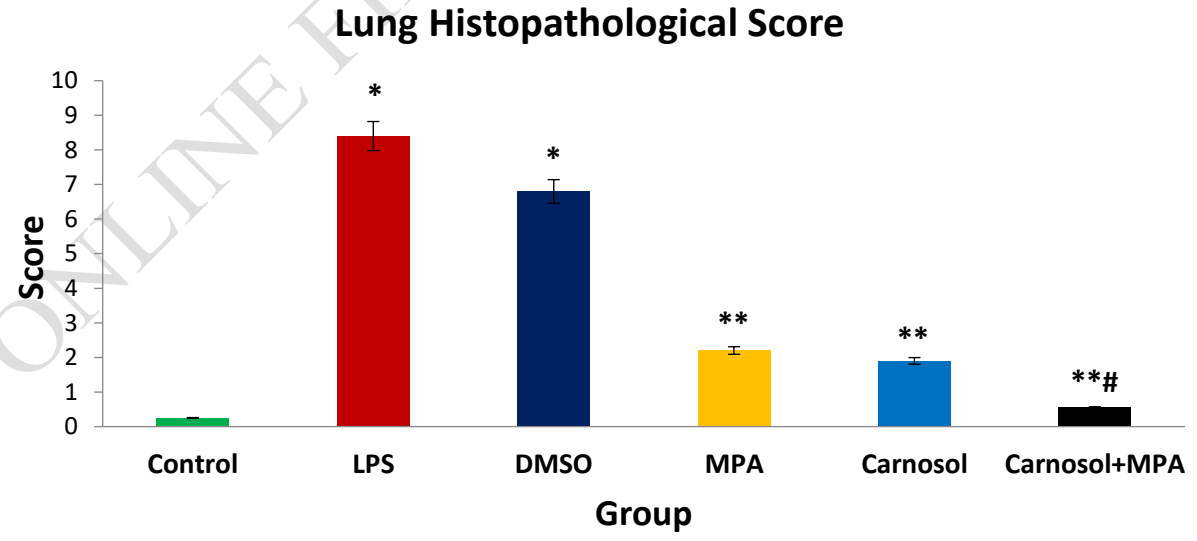

Fig. 5. Impact of the tested agents on lung histological scoring, data are reflected as mean±SD, * – indicates a remarkable difference vs. the control group ($p<0.05$), ** – indicates a remarkable difference vs. the LPS and DMSO groups ($p<0.05$), and # – indicates a remarkable difference vs. the carnosol and/or MPA group ($p<0.05$)

Preventive effect of tested agents on lung histopathological changes

In the healthy control group, lung histology demonstrated a well-maintained pulmonary architecture, characterized by intact alveolar structures and preserved capillary endothelium. Only minimal, nonspecific inflammatory changes were evident (Figure 6A). Conversely, the LPS-induced group showed extensive pathological damage, including intense acute inflammation, prominent vascular congestion, disruption of capillary integrity, thickening of alveolar septa, reduction of airspace volume, and hyaline membranes formation (Figure 6B).

In the DMSO group, lung histology demonstrated an acute inflammatory process of moderate to severe degree, with mild congestion of blood vessels, diffuse alveolar wall thickening, and areas of capillary breakdown with hyaline membrane deposition, as clarified in Figure 7A. Tissue samples from the MPA group enjoyed minimal inflammatory involvement, featuring localized blood vessel engorgement, irregular enlargement of the alveolar septa, disruption of capillary structures, and occasional accumulation of hyaline membranes, accompanied by a slight narrowing of the airspaces as explained in Figure 7B.

Lung histology from the carnosol group indicated intact alveolar walls and capillaries, lacking any vascular congestion or inflammation as seen in Figure 8A. Likewise, tissues from the Carnosol+MPA group displayed normal lung structure, including clear alveoli and no evidence of inflammation, congestion, or hyaline membranes as described in Figure 8B.

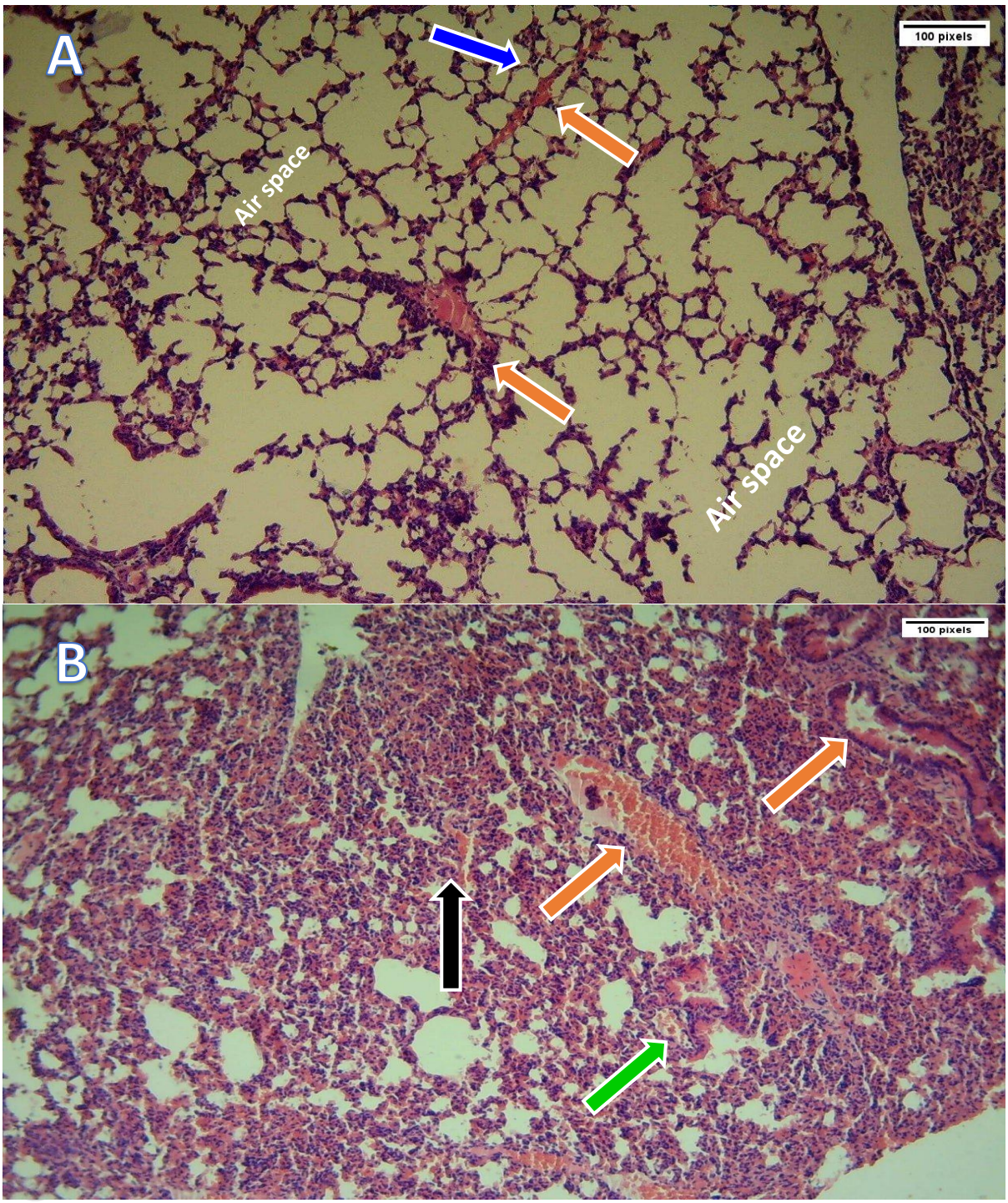

Fig. 6. Representative lung histology of control and LPS-treated mice, A: The control group showing intact alveolar architecture (blue arrow), B: LPS group demonstrating severe inflammatory infiltration (black arrow), vascular congestion (red arrow), septal thickening, and hyaline membranes (green arrow), photomicrographs captured at 10× magnification (H&E stain, scale bar=100 µm)

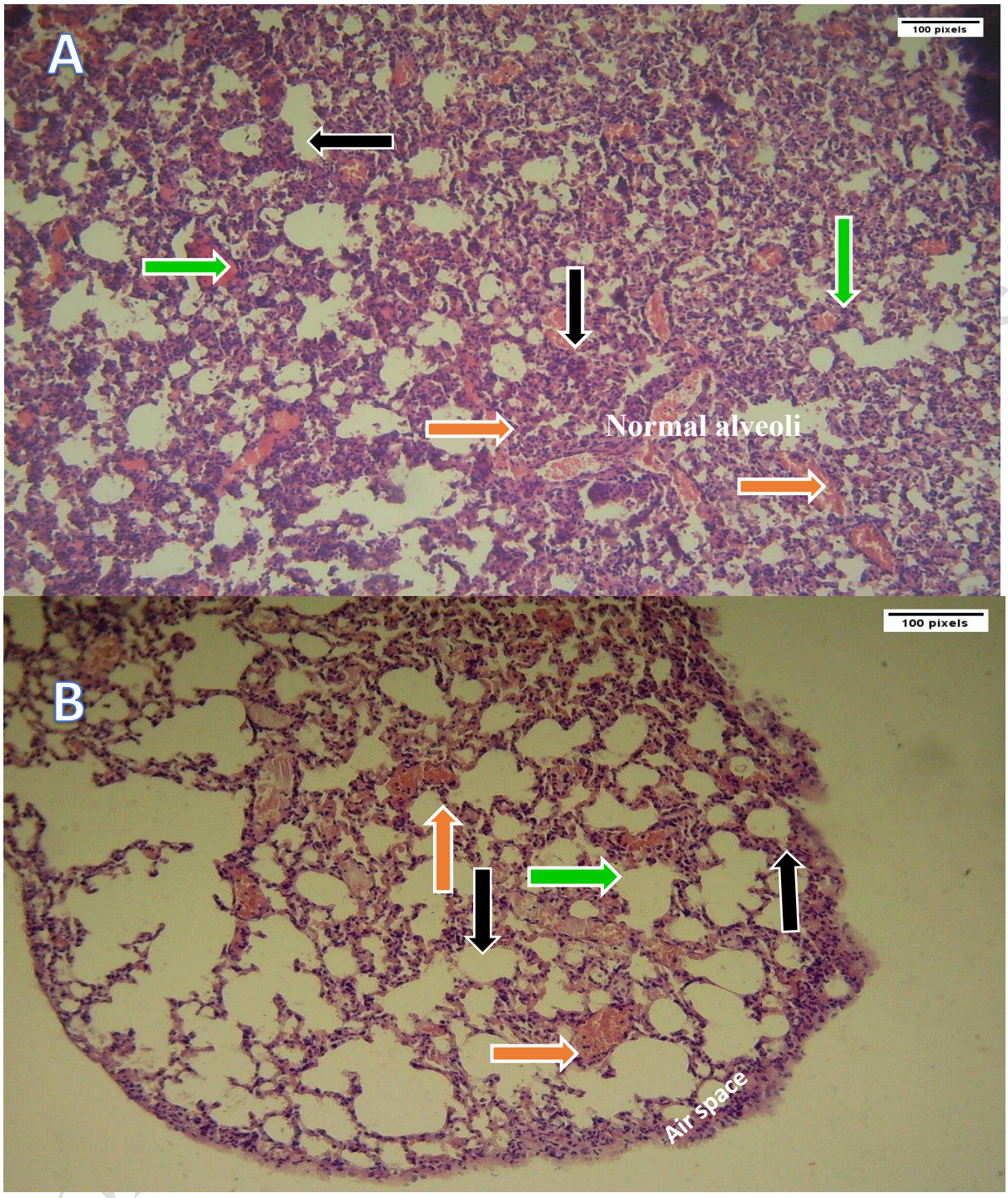

Fig. 7. Histological analysis of lung tissue in DMSO and MPA groups, A: The DMSO group showing moderate-to-severe inflammation (black arrow), mild congestion (red arrow), septal thickening, and hyaline membranes (green arrow), B: MPA-treated group exhibiting mild inflammatory changes (black arrow), scattered vascular congestion (red arrow), focal alveolar thickening, and partial hyaline deposition (green arrow), photomicrographs captured at 10× magnification (H&E stain, scale bar=100 µm)

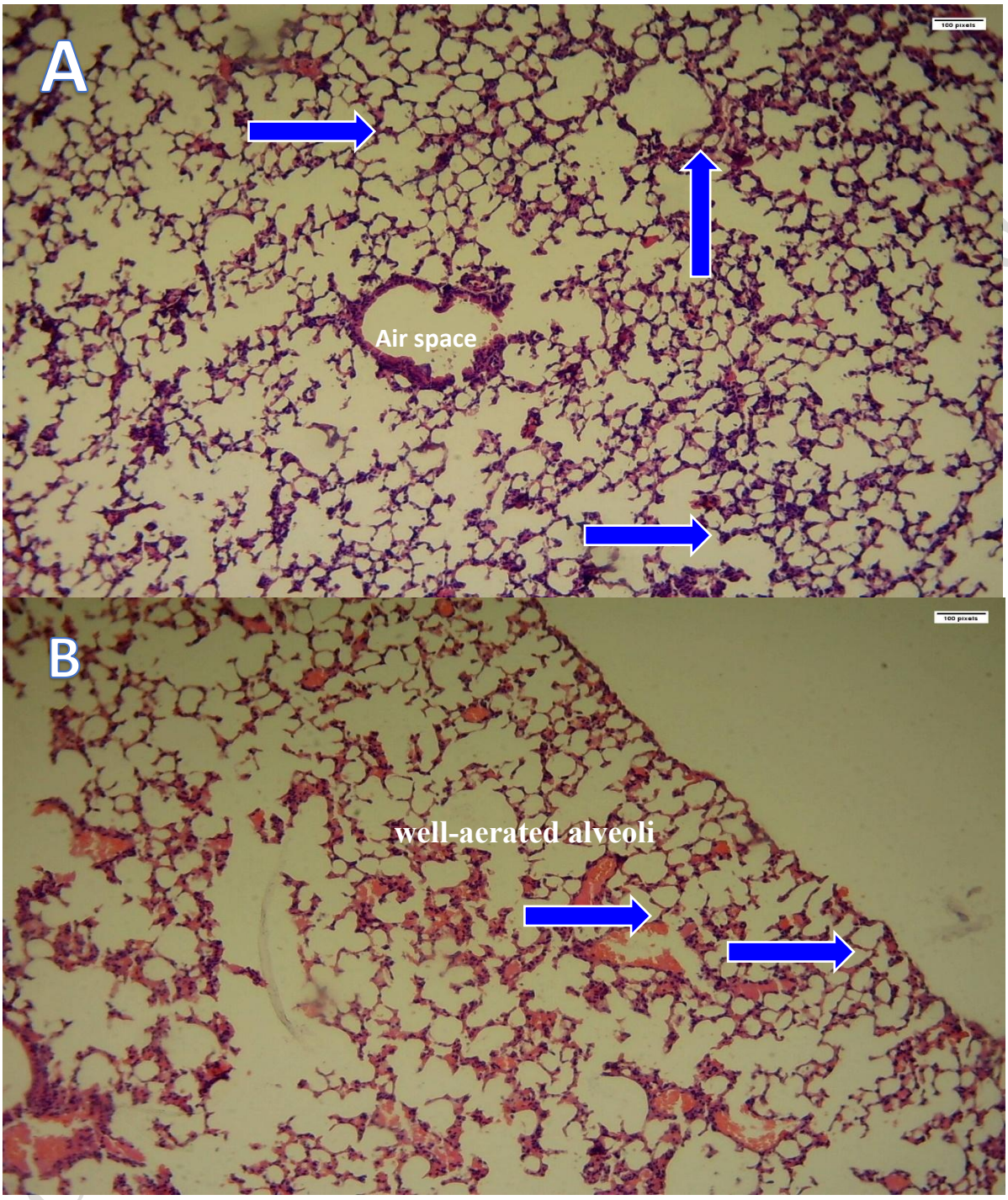

Fig. 8. Lung tissue morphology in CAR- and CAR+MPA-treated mice, A: CAR group displaying preserved alveolar structure (blue arrow), intact capillaries, and absence of inflammation or congestion, B: CAR+MPA group showing well-aerated alveoli, normal septal thickness, and no pathological alterations, photomicrographs captured at 10× magnification (H&E stain, scale bar=100 µm)

Discussion

Cytokine storm induction

Hypercytokinemia is an uncontrolled systemic inflammatory response typically driven by bacterial or viral infections and is accompanied by overproduction of inflammatory cytokines. In our study, intraperitoneal LPS challenge caused severe pulmonary inflammation with a marked increase in IL-1β, IL-6, and TNF-α levels. This experimental model is widely accepted to mimic critical biochemical and histopathological criteria of acute lung inflammatory injury, and it has served as a consistent tool for the testing of anti-inflammatory agents.[40] Although cytokine storm has been associated with severe pathologies such as sepsis and ARDS, the present results must be viewed within a meticulously managed preclinical animal model.

Preventive effects of tested agents on IL-1 β IL-6, and TNF-α level in LPS-induced cytokine storm in mice

The findings of this investigation indicated LPS provoked an extensive pulmonary inflammatory response characterized by the highest levels of IL-1β, IL-6, and TNF-α. These cytokines are critical intermediaries for the cytokine storm and have important functions in propagating inflammatory cascades and leukocyte recruitment as well as tissue injury in experimental models of acute lung inflammation.[41] Treatment with either carnosol, MPA, or their combination substantially suppressed the increments of LPS-induced cytokines. The demonstrated IL-1β inhibition is of particular interest because this cytokine is produced after TLR4 stimulation and inflammasome-dependent processing, participating in the enhancement of subsequent cytokine release.[42,43] Downregulation of IL-1β after carnosol exposure is also in line with findings reporting that carnosol inhibits synthesis of pro-inflammatory cytokines such as IL-1β, IL-6, and TNF-α from activated immune cells.[44,45]

IL-6, a key biomarker in the pathogenesis of cytokine storm and systemic inflammation, exhibited a notable increase after the LPS challenge. Similar results in experimental models have shown that IL-6 is a principal modulator of cytokine cascade activation involving the hyperinflammatory state.[40,46] However, a prominent decrease in IL-6 was apparent following the treatment protocol with carnosol, MPA, or their combination. Of note, the combined administration of carnosol with MPA was more effective in the downregulation of IL-6 than either agent alone. The carnosol-mediated attenuation of IL-6 levels is supported by earlier data showing that this phytochemical exerts wide anti-inflammatory actions, owing to its capacity to dampen macrophage activation during cytokine storms and to block major inflammatory response regulators like IL-6, TNF-α, and IL-1β.[47] Although we did not explore the intracellular signaling pathways in the current study, it has been demonstrated in other works that carnosol effects on IL-6 are related to NF-κB and MAPK antagonism or through stimulating PPAR-γ–dependent anti-inflammatory axis.[48,49] Such mechanisms are well described in inflammatory models and could give a justification for the noticed diminution in cytokines. Likewise, TNF-α expression dramatically rose after LPS exposure and diminished with carnosol and MPA interventions. TNF-α is a proximal mediator of cytokine storms and significantly contributes to endothelial dysfunction and tissue damage.[50-52] Former experimental observations revealed that carnosol and related

polyphenolic constituents hinder generation of TNF-α, IL-1β, and IL-6 through interfering with transactivation of pro-inflammatory genes and modulating activated macrophages.[53,54] Although these pathways were not assayed in our experiment, the differences among treatment groups would suggest that carnosol exerts an anti-inflammatory effect detected by other authors using different preclinical models[55,56]
Remarkably, combined carnosol plus MPA led to higher mitigation of IL-6 and TNF-α values at individual dosages of both agents, hinting at a putative synergistic anti-inflammatory activity under this experimental setting. This finding is preliminary and is valid only for the current animal model since there was no pharmacodynamic or dose-saving study carried out.
Taken together, these results demonstrate the effective alleviation of LPS-evoked cytokine storm by carnosol through downregulation of pivotal proinflammatory mediators. When used in combination with MPA, carnosol can even potentiate cytokine suppression without evidence of additional toxicity, indicating that it could be a supplemental anti-inflammatory agent in experimental models of cytokine storm.

Effects of tested compounds on histopathological analysis

Following the LPS challenge, severe lung histopathological changes were observed, such as inflammatory cell infiltrates, vascular congestion, thickening of alveolar septal walls, and hyaline membrane formation, which are typical features of acute lung injury described in earlier investigations.[57,58] These histological aberrations are a reflection of downstream tissue effects secondary to the overproduction of cytokines.
Carnosol, MPA, and Carnosol+MPA-treated animals revealed noteworthy diminution in lung injury scores and maintenance of alveolar architecture. These results are in line with previous efforts describing the pulmonoprotective activities of carnosol against experimental lung injury.[59,60]
According to related literature, the proposed histological amelioration might be attributed to reduced generation of inflammatory mediators and oxidative stress, events that were not directly proved in our current work.[61,62]
Use of a standardized histopathological scoring system, blinded evaluation, and assessment of multiple tissue regions supports the robustness of these findings and allows comparison with existing grading systems for acute lung injury.

Comparative effects of carnosol and MPA

While both carnosol and MPA share the pharmacological ability to ameliorate LPS-induced cytokine storms, their working mechanisms are fundamentally distinct. MPA is a synthetic glucocorticoid that exerts its effects mainly by means of glucocorticoid receptor-mediated transcriptional repression, resulting in wide-range inhibition of immune cell activation and cytokine secretion[16,24]. Although efficient in combating inflammation, this phenomenon is accompanied by systemic immunosuppression and potential complications such as increased risk of infection and metabolic abnormalities.[63,64] Conversely, carnosol, a

nature-derived polyphenolic diterpene, displays anti-inflammatory properties due to its exclusive ability to target some critical intracellular signaling pathways, such as activation of PPAR-γ, reduction in MAPK phosphorylation, and suppression of NF-κB-dependent activity, accompanied by a reduction in the transcription of pro-inflammatory cytokines (TNF-α, IL-6, and IL-1β), as well as strengthening antioxidant defenses with lipid peroxidation inhibition.[65,66] Such focused management might explain how carnosol is able to suppress exaggerated inflammatory reactions without the generalized systemic immunosuppression typically observed with corticosteroids, thus offering a potentially safer therapeutic profile.[23,48]

Study limitations

This study has several limitations. First, it was conducted using an LPS-evoked cytokine storm model in mice, which may not fully replicate the complexity of human hyper-inflammatory conditions, including COVID-19-related cytokine storms. Second, treatments were administered for only 7 days, so long-term outcomes and potential delayed effects of carnosol and combination therapy were not assessed. Third, the study focused primarily on lung tissue, and systemic effects on other organs commonly affected by cytokine storm, such as the liver, kidneys, and heart, were not evaluated. Importantly, while our biochemical and histological analyses provide indirect evidence of anti-inflammatory activity, the absence of mechanistic assays targeting key pathways such as NF-κB, MAPK, and PPAR-γ, together with the lack of pharmacokinetic and dosage–response studies and a formal toxicity evaluation, constrains the depth of interpretation. Future studies are warranted to address these aspects and to further elucidate the molecular mechanisms underlying carnosol therapeutic potential. Finally, only a single dose of carnosol and MPA and one combination regimen were tested, highlighting the need for further studies to optimize dosing strategies and assess potential toxicity at varying concentrations. The subsequent evaluation may also include distribution-sensitive representations that offer more insights into the flow of data and deep patterns.

Conclusion

In this murine model of LPS-evoked cytokine storm, carnosol remarkably decreased the levels of pulmonary pro-inflammatory cytokines (IL-1B, IL-6, and TNF-α) and mitigated lung histopathological alterations. The co-administration of carnosol and MPA resulted in a more profound amelioration of the tested inflammatory biomarkers compared to either treatment alone under these experimental settings. These observations offer preclinical evidence that carnosol demonstrates anti-inflammatory and pneumoprotective properties in acute inflammation of the lung. Interpretation of the observed effects of combined therapy should be cautious and restricted to the current animal model, consistent with no clinical or dose-sparing advantage. Still, additional investigations are warranted to clarify the mechanisms, dose–response correlations, and translational potential of carnosol alone or combined with corticosteroids in various experimental contexts.

Acknowledgements

The results of this study constitute a fundamental part of a PhD thesis submitted to the Department of Pharmacology, College of Medicine, Al-Nahrain University.

Declarations

Funding

The research did not receive any external or commercial funding.

Author contributions

Conceptualization, A.F.A.M., A.R.A.R., and H.R.-S.; Methodology, A.F.A.M.; Software, H.R.-S., M.R.S., and M.N.H.; Validation, A.R.A.R., H.R.-S., and F.M.A.; Formal Analysis, A.F.A.M. and M.N.H.; Investigation, F.M.A. and M.N.H.; Resources, A.F.A.M. and M.R.S.; Data Curation, F.M.A. and M.R.S.; Writing – Original Draft Preparation, A.F.A.M..; Writing – Review & Editing, A.R.A.R. and H.R.-S.; Visualization, A.R.A.R. and H.R.-S.; Supervision, A.R.A.R.; Project Administration, F.M.A., M.R.S., and M.N.H.; Funding Acquisition, A.F.A.M.

Conflicts of interest

The authors declare no conflicts of interest related to this research.

Data availability

The data supporting the findings of this study are available from the corresponding author upon reasonable request.

Ethics approval

The Institutional Review Board (IRB) of Al-Nahrain University, College of Medicine, approved this study on November 21, 2021, with Approval No. 20215951. All animal procedures adhered to the 3Rs (Replacement, Reduction, and Refinement) ethical rules to lessen animal use and suffering. Humane endpoints were defined, and analgesia was deployed to relieve pain or discomfort as needed.

References

1. Feuillet V, Canard B, Trautmann A. Combining antivirals and immunomodulators to fight COVID-19. *Trends Immunol*. 2021;42(1):31-44. doi:10.1016/j.it.2020.11.003
2. Al-Saray D, Al-Asady FM, Tuhair T. Role of antibodies against SARS-CoV-2 in the detection of coronavirus, its transmissibility and immunological status determination among different

populations in Babylon Province. *Open Access Maced J Med Sci.* 2022;10(A):644-649. doi:10.3889/oamjms.2022.9372

3. Picchianti Diamanti A, Rosado MM, Pioli C, Sesti G, Laganà B. Cytokine release syndrome in COVID-19 patients: a new scenario for an old concern. *Int J Mol Sci*. 2020;21(9):3330. doi:10.3390/ijms21093330
4. Omran T, Al-Asady FM, Sajit EJ, Al-Saadi H. Assessment of D-dimer level and C-reactive protein in correlation with CT findings in positive PCR–COVID-19 patients. *Malays J Microbiol.* 2025;21(1):135-142. doi:10.21161/mjm.230200
5. Al-Taie SF, Fedwi MM, Merza M, et al. Evaluation of different sedation scales in the ICU management of COVID-19 patients. *Sci Rep*. 2025;15(1):28782. doi:10.1038/s41598-025-14421-1
6. Kozlov EM, Ivanova E, Grechko AV, et al. Involvement of oxidative stress and the innate immune system in SARS-CoV-2 infection. *Diseases.* 2021;9(1):17. doi:10.3390/diseases9010017
7. Al-Asady FM, Omran TZ, Abood FM. Humoral immunity role in diagnosis of COVID-19 among people visited a tertiary care hospital in Hilla City. *Med J Babylon.* 2023;20(3):497-502. doi:10.4103/MJBL.MJBL_124_23
8. Ayad ZM, Al-Ameedi AI, Hajwal SK, et al. Relationship between paediatric antibiotic misuse and recurrent acute respiratory tract infection. *Pharmakeftiki.* 2025;37(2 suppl):193-197. doi:10.60988/p.v37i2S.188
9. Luty RS, Abbas SF, Haji SA, Ridha-Salman H. Hepatoprotective effect of catechin on acetaminophen-induced liver injury in rats. *Comp Clin Pathol.* 2025;34(4):705-718. doi:10.1007/s00580-025-03682-x
10. Yahiya YI, Hadi NR, Abu Raghif A, et al. Protective effect of IAXO-102 on renal ischemia-reperfusion injury in rats. *J Med Life.* 2023;16(4):623-630. doi:10.25122/jml-2022-0280
11. Raheem AK, Abu-Raghif AR, Abbas AH, et al. Quercetin mitigates sepsis-induced renal injury via inhibition of inflammatory and oxidative pathways in mice. *J Mol Histol.* 2025;56(3):184. doi:10.1007/s10735-025-10442-2
12. Raheem AKK, Abu-Raghif AR, Zigam QA. Cilostazol protects against sepsis-induced kidney impairment in a mouse model. *J Med Chem Sci.* 2023;6(5):1193-1203. doi:10.26655/jmchemsci.2023.5.25
13. Aal-Aaboda M, Abu Raghif AR, Hadi NR. Effect of lipopolysaccharide from *Rhodobacter sphaeroides* on inflammatory pathways and oxidative stress in renal ischemia-reperfusion injury in rats. *Arch Razi Inst.* 2021;76(4):1013-1024. doi:10.22092/ari.2021.356003.1761

14. Shareef SM, Kathem SH, Ridha-Salman H. L-carvone alleviates lipopolysaccharide-induced acute kidney injury via modulation of MyD88-dependent and independent signaling pathways in mice. *Mol Biol Rep.* 2025;53(1):39. doi:10.1007/s11033-025-11213-8
15. Montazersaheb S, Hosseiniyan Khatibi SM, Hejazi MS, et al. COVID-19 infection: an overview on cytokine storm and related interventions. *Virol J.* 2022;19(1):92. doi:10.1186/s12985-022-01814-1
16. Coutinho AE, Chapman KE. Anti-inflammatory and immunosuppressive effects of glucocorticoids: recent developments and mechanistic insights. *Mol Cell Endocrinol.* 2011;335(1):2-13. doi:10.1016/j.mce.2010.04.005
17. Farooq Ali B, Abu-Raghif AR, Ridha-Salman H. Protective effect of cinnarizine on imiquimod-induced psoriasis in mice. *J Res Pharm.* 2025;29(4):1783-1791. doi:10.12991/jrespharm.1734970
18. Obaid SH, Gatea FK. Effect of kaempferol, amygdalin, and methylprednisolone alone and in combination in induced cytokine storm in mice. *Acta Pharm Sci.* 2024;62(4):735-747. doi:10.23893/1307-2080.APS6248
19. Al-Jabr KH, Alhumaidan LS, Alghamdi AA, et al. Awareness of side effects of corticosteroids among users and nonusers in Saudi Arabia. *J Pharm Bioallied Sci.* 2024;16(suppl 2):S1612-S1618. doi:10.4103/jpbs.jpbs_925_23
20. Wang L, Waltenberger B, Pferschy-Wenzig EM, et al. Natural product agonists of peroxisome proliferator-activated receptor gamma (PPARγ): a review. *Biochem Pharmacol.* 2014;92(1):73-89. doi:10.1016/j.bcp.2014.07.018
21. Al-Rajhi SH, Shihab EM, Ridha-Salman H, et al. Protective effect of combined glutathione and prednisolone administration in LPS-induced cytokine storm in mice. *Pharmakeftiki.* 2025;37(2 suppl):122-126. doi:10.60988/p.v37i2S.157
22. Poeckel D, Greiner C, Verhoff M, et al. Carnosic acid and carnosol inhibit human 5-lipoxygenase and suppress pro-inflammatory responses. *Biochem Pharmacol.* 2008;76(1):91-97. doi:10.1016/j.bcp.2008.04.013
23. Maione F, Cantone V, Pace S, et al. Anti-inflammatory and analgesic activity of carnosol and carnosic acid. *Br J Pharmacol.* 2017;174(11):1497-1508. doi:10.1111/bph.13545
24. Tariq ZT, Abu-Raghif AR, Raheem AK, et al. Huperzine A versus epicatechin in LPS-induced lung injury in mice. *Pharmakeftiki.* 2025;37(2 suppl). doi:10.60988/p.v37i2S.244
25. Aal-Aaboda M, Raghif ARA, Almudhafer RH, Hadi NR. Lipopolysaccharide from *Rhodobacter sphaeroides* modulates toll-like receptor expression in renal ischemia-reperfusion injury. *J Med Life.* 2022;15(5):685. doi:10.25122/jml-2021-0255
26. Abed-Mansoor A, Abu-Raghif AR. Attenuated effects of rivastigmine in induced cytokine storm in mice. *J Emerg Med Trauma Acute Care.* 2022;2022(3):12. doi:10.5339/jemtac.2022.ismc.12

27. Shi W, Xu G, Zhan X, et al. Carnosol inhibits inflammasome activation by targeting HSP90. *Cell Death Dis.* 2020;11(4):252. doi:10.1038/s41419-020-2460-x
28. Al-Naimi MS, Abu-Raghif AR, Fawzi HA. Rifaximin combined with methylprednisolone attenuates LPS-induced inflammation in mice. *Toxicol Rep.* 2024;13:101808. doi:10.1016/j.toxrep.2024.101808
29. Sadiq A, Zalzala M. Protective effect of safranal on LPS-induced acute lung injury in mice. *Int J Drug Deliv Technol.* 2021;11:771-776. doi:10.25258/ijddt.11.3.19
30. Shao C, Lin S, Liu S, et al. HIF-1α-induced glycolysis in macrophages during endotoxemia. *Oxid Med Cell Longev.* 2019;2019:7136585. doi:10.1155/2019/7136585
31. AlBairmani RJH, Shihab EM, Ridha-Salman H, et al. D-limonene attenuates D-galactose-induced skin aging in mice. *J Mol Histol.* 2025;56(6):364. doi:10.1007/s10735-025-10654-6
32. Sharif SJ, Kadhim HM, Ahmed BS, et al. Gastroprotective effects of emodin in diclofenac-induced gastric ulceration in rats. *Naunyn Schmiedebergs Arch Pharmacol.* 2025. doi:10.1007/s00210-025-04701-y
33. Tofiq SH, Idan HM. Hematological assessments of children with oral aphthous ulcer. *J Appl Hematol.* 2024;15(2):111-115. doi:10.4103/joah.joah_23_24
34. Idan HM, Hasani RA-M, Othman IQ. Effect of anemia on oral cavity and hematological assessments. *Diyala J Med*. 2024;26(1):153-162. doi:10.26505/djm.v26i1.1087
35. Hassan SF, Abu Raghif AR, Kadhim EJ, et al. Phenolic components of Iraqi sumac (*Rhus coriaria*): antioxidant and hepatoprotective effects. *Eur J Clin Exp Med*. 2025;23(3):1-24. doi:10.15584/ejcem.2025.3.29
36. Abbod MS, Al-Jawad FH, Anoze AA, et al. Antiatherosclerotic effect of L-thyroxine and verapamil in rabbits. *Int J Pharm Sci Rev Res*. 2014;27(1):254-260.
37. Hussein MN, Abu-Raghif AR, Ridha-Salman H, et al. Flavonoids from *Conyza canadensis* mitigate atopic dermatitis in mice. *Comp Clin Pathol*. 2025;34(5):987-1010. doi:10.1007/s00580-025-03709-3
38. Hulse EJ, Smith SH, Wallace WA, et al. Development of a pulmonary histopathology scoring system. *PLoS One*. 2020;15(10):e0240563. doi:10.1371/journal.pone.0240563
39. Daniel WW, Cross CL. Biostatistics: a foundation for analysis in the health sciences. Hoboken, NJ: John Wiley & Sons; 2018.
40. Tang Y, Liu J, Zhang D, et al. Cytokine storm in COVID-19: evidence and treatment strategies. *Front Immunol*. 2020;11:1708. doi:10.3389/fimmu.2020.01708
41. Al-Ani B, ShamsEldeen AM, Kamar SS, et al. Lipopolysaccharide-induced acute lung injury in a rat model of COVID-19. *Clin Exp Pharmacol Physiol*. 2022;49(4):483-491. doi:10.1111/1440-1681.13620

42. Dinarello CA. IL-1β as the gatekeeper of inflammation. *Eur J Immunol*. 2011;41(5):1203-1217. doi:10.1002/eji.201141550
43. Schroder K, Tschopp J. The inflammasomes. *Cell.* 2010;140(6):821-832. doi:10.1016/j.cell.2010.01.040
44. Chen J, Sun N, Li F, et al. Carnosol alleviates collagen-induced arthritis. *Biomed Res Int*. 2023;2023:1179973. doi:10.1155/2023/1179973
45. Lee JE, Im DS. Suppressive effect of carnosol on ovalbumin-induced allergic asthma. *Biomol Ther.* 2021;29(1):58-63. doi:10.4062/biomolther.2020.050
46. Ishijima T, Nakajima K. Induction of TNF-α, IL-1β, and IL-6 in endotoxin-stimulated microglia. *Sci Prog*. 2021;104(4):00368504211054985. doi:10.1177/00368504211054985
47. Sapra L, Bhardwaj A, Azam Z, et al. Phytotherapy for cytokine storm in COVID-19. *Front Biosci (Landmark Ed)*. 2021;26(5):51-75. doi:10.52586/4924
48. Gazzillo E, Saviano A, Raucci F, et al. Carnosol modulates mPGES-1/PPAR-γ axis. *Biomed Pharmacother.* 2025;191:118407.
49. Li L, Pan Z, Ning D, et al. Rosmanol and carnosol alleviate rheumatoid arthritis. *Molecules*. 2021;27(1):78. doi:10.3390/molecules27010078
50. Kadhim HM, Al-Mosawi AM. Effects of emodin and salvianolic acid on lung fibrosis. *Int J Drug Deliv Technol*. 2021;11(4):1269-1274. doi:10.25258/ijddt.11.4.25
51. Zein L, Grossmann J, Swoboda H, et al. Haptoglobin buffers lipopolysaccharides. *Front Immunol*. 2024;15:1401527.
52. Shareef SM, Kathem SH, Ridha-Salman H. L-carvone protects against sepsis-associated renal injury. *J Taibah Univ Med Sci*. 2026;21(1):49-66. doi:10.1016/j.jtumed.2025.12.008
53. Habtemariam S. Anti-inflammatory mechanisms of rosemary diterpenes. *Biomedicines*. 2023;11(2):545. doi:10.3390/biomedicines11020545
54. Schwager J, Hoeller U, Wolfram S, et al. Carnosol modulates cytokine production. *Molecules*. 2016;21(4):465. doi:10.3390/molecules21040465
55. Chen CC, Chen HL, Hsieh CW, et al. Nrf2-dependent glutathione induction by carnosol. *Acta Pharmacol Sin*. 2011;32(1):62-69. doi:10.1038/aps.2010.181
56. Lee DY, Hwang CJ, Choi JY, et al. Carnosol inhibits phthalic anhydride-induced dermatitis. *Biomol Ther*. 2017;25(5):535-544. doi:10.4062/biomolther.2017.006
57. Bhargava R, Janssen W, Altmann C, et al. Intratracheal IL-6 in acute lung injury. *PLoS One*. 2013;8(5):e61405. doi:10.1371/journal.pone.0061405
58. Fan H, Cook JA. Molecular mechanisms of endotoxin tolerance. *J Endotoxin Res*. 2004;10(2):71-84. doi:10.1179/096805104225003997

59. Ciavarella C, Motta I, Valente S, et al. PPAR-γ agonists for cytokine storm modulation. *Molecules*. 2020;25(9):2076. doi:10.3390/molecules25092076
60. Zhang YA, Li FW, Dong YX, et al. PPAR-γ regulates macrophage polarization. *FASEB J*. 2024;38(8):e23613.
61. Li Q, Liu L, Sun H, et al. Carnosic acid protects against acute lung injury. *Exp Ther Med*. 2019;18(5):3707-3714. doi:10.3892/etm.2019.8042
62. Tian XF, Yao JH, Zhang XS, et al. Protective effect of carnosol on lung injury. *Surg Today*. 2010;40(9):858-865. doi:10.1007/s00595-009-4170-y
63. Fernandes RM, Wingert A, Vandermeer B, et al. Safety of corticosteroids in children. *BMJ Open*. 2019;9(8):e028511. doi:10.1136/bmjopen-2018-028511
64. Abbas AH, Hassan ZM, Albarki MA, et al. Cimifugin and vinpocetine in psoriasis-like model. *Pharmakeftiki*. 2025;37(2S). doi:10.60988/p.v37i2S.134
65. Kashyap D, Kumar G, Sharma A, et al. Mechanistic insight into carnosol pharmacology. *Life Sci*. 2017;169:27-36. doi:10.1016/j.lfs.2016.11.013
66. Singh D, Mittal N, Siddiqui M. Pharmacological potentials of phenolic diterpenes from *Rosmarinus officinalis*. *Trends Phytochem Res*. 2023;7(3):156-169. doi:10.30495/tpr.2023.1990761.1365